Applied
Organometallic
Chemistry

Received: 27 March 2008 Accepted: 17 April 2008

(www.interscience.com) DOI 10.1002/aoc.1422

Synthesis and properties of N_3 and CN delivery compounds and related precursors for nitride and ceramic fabrication

Jesse B. Tice, C. J. Ritter, A. V. G. Chizmeshya, Brandon Forrest,
Levi Torrison, T. L. Groy and J. Kouvetakis*

The simple azido and cyano compounds Cl_2AsN_3, Br_2AsN_3, $(C_6H_5)SiH_2N_3$, $(C_6H_5)SiH_2CN$ and *p*-(tolyl)SiH_2CN have been prepared for the first time by metathesis reactions involving the corresponding halides and NaN_3, LiN_3 and LiCN. These compounds represent a highly reactive and efficient family of delivery reagents for the preparation of N_3 and CN molecular precursors to bulk ceramics and nitride thin films. They are isolated as low volatility liquids and characterized by spectroscopic methods and chemical analysis. *Ab initio* simulations were used to elucidate the structural and vibrational properties of the simpler, fully inorganic Cl_2AsN_3 and Br_2AsN_3 species. This theoretical treatment was extended to include the hypothetical H_2AsN_3 and $HClAsN_3$ derivatives which are particularly desirable as single-source low-temperature As–N sources for the formation of highly sought after, metastable $GaAs_{1-x}N_x$ materials for solar cell applications. The practical utility of the title molecules is also demonstrated by synthesizing several representative compounds of B, Be, Ga and Al, which are of interest for the development of open frameworks, optoelectronic nitrides and refractory B–C–N hybrids. The cyanide derivatives $(C_6H_5)SiH_2CN$ and *p*-(tolyl)SiH_2CN react readily with Be and B halides to yield crystalline $Be(CN)_2$ and amorphous B–C–N. The latter is crystallized upon heating to form graphite-like polymorphs with homogeneous nanoscale morphologies. The azide derivatives Cl_2AsN_3, Br_2AsN_3 and $(C_6H_5)SiH_2N_3$ react readily with $GaBr_3$, $GaCl_3$ and BBr_3 to produce high yields of the previously reported Br_2GaN_3, Cl_2GaN_3 and Br_2BN_3, respectively. The latter is shown to possess a trimeric molecular structure in which the α-nitrogen of the azide group bridges the boron atoms to form cyclohexane-like B_3N_3 rings.

Keywords: azides; cyanides; arsenic, silicon; GaAsN semiconductors; framework solids

Introduction

Silyl azides and cyanides, such as trimethylsilyl azide, Me_3SiN_3 and trimethylsilyl cyanide, Me_3SiCN ($Me = CH_3$), have long been known as extremely useful and highly versatile reagents in organic and inorganic synthesis. In particular, their use in the synthesis of metal/metalloid azides and cyanides of the main group is well documented.[1] It has been shown that Me_3SiN_3 produces stable 1 : 1 adducts with $GaCl_3$ and $GaBr_3$ with the general formula $[Me_3SiN_3]GaX_3$ (X = Cl, Br). These disproportionate thermally by a simple nucleophilic substitution process, to form the X_2GaN_3 and Me_3SiX byproducts according to eqn (1):

$$[Me_3SiN_3] \bullet GaX_3 \longrightarrow X_2GaN_3 + Me_3SiX \quad (X = Cl, Br) \qquad (1)$$

The Cl_2GaN_3 compound is obtained by heating the adduct in vacuum at 50 °C and has been used to deposit high-quality, heteroepitaxial GaN layers between 600 and 700 °C.[2] Similarly, Br_2GaN_3 is isolated at slightly higher temperatures and is subsequently used to prepare H_2GaN_3 and D_2GaN_3. The latter serves as an ideal precursor for growth of GaN and AlGaN alloys at unprecedented low temperatures ranging from 150 to 550 °C.[3] A major issue with the Br_2GaN_3, obtained via this method, is that it often lacks the necessary purity to be used routinely and safely as a reliable starting material. For instance, impurities in the compound can lead to the formation of potentially explosive byproducts in D_2GaN_3, thus limiting its practical value.

Our search for alternative sources to the Me_3SiN_3 azide which do not form stable adducts with $GaBr_3$ and would potentially afford a more direct and efficient route to high-purity Br_2GaN_3, and other related azides such as Cl_2GaN_3 and Br_2BN_3 led to the synthesis of Cl_2AsN_3, Br_2AsN_3 and $(C_6H_5)SiH_2N_3$ (see Fig. 1). The As compounds incorporate weakly bonded As–N_3 functionalities specifically designed to react at low temperatures with metal halides to form the corresponding azides via complete elimination of stable AsX_3 byproducts. For the $(C_6H_5)SiH_2N_3$ compound the electronic ligand field around Si is altered to enhance elimination of organometallic halide $(C_6H_5)SiH_2X$ byproducts, leading to facile formation of the target high-purity products in practical yields. These strategies circumvent the formation of any undesirable intermediates such as the $[Me_3SiN_3] \bullet GaX_3$ shown in eqn (1). The use of less electronically donating ligands such as phenyl and H-groups (in contrast to methyl groups) on Si may render this element substantially more electron-deficient and thus more susceptible to nucleophilic attack.

In this connection, cyanide derivatives of the $(C_6H_5)SiH_2N_3$ species such as $(C_6H_5)SiH_2CN$ and *p*-(tolyl)SiH_2CN (see Fig. 1) represent a completely analogous class of starting materials that could be ideally suited for the preparation of framework metal

---

* Correspondence to: J. Kouvetakis, Department of Chemistry and Biochemistry, Arizona State University, PO Box 871604, Tempe, AZ 85287, USA.
E-mail: jkouvetakis@asu.edu

Department of Chemistry and Biochemistry, Arizona State University, Tempe, AZ 85287, USA

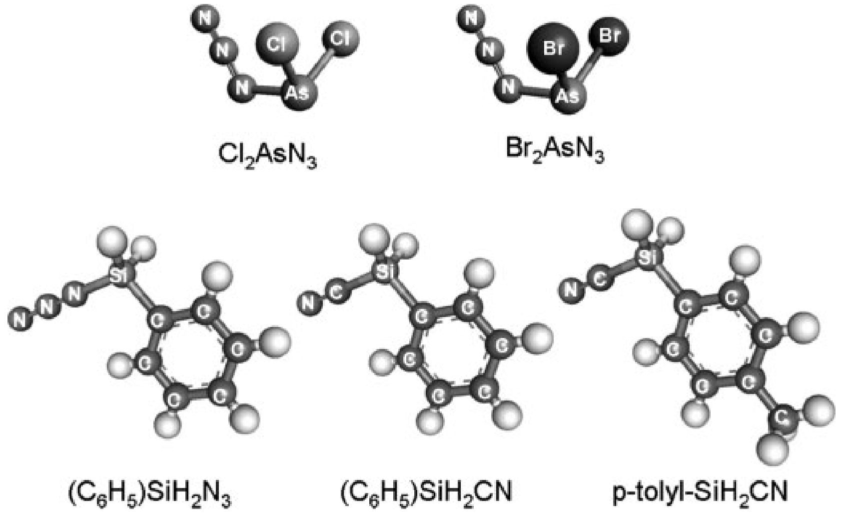

Figure 1. Structural representations of Cl_2AsN_3, $(C_6H_5)SiH_2N_3$, $(C_6H_5)SiH_2CN$ and *p*-(tolyl)SiH_2CN. Hydrogen atoms are represented by white spheres.

cyanides with composition $M(CN)_3$ or $M(CN)_2$ [M = Al, Ga, In, Be]. These are of interest in topical and emerging technological areas such as hydrogen storage for renewable energy, negative thermal expansion (NTE) applications and precursors to superhard ultrastrong light element ceramics. Here we synthesize these compounds by adopting a parallel procedure to the one described above and explore their utility in facile CN^- delivery via reactions with metal halides. As a proof of concept demonstration, these compounds are reacted with $BeCl_2$ to directly yield crystalline nano-porous $Be(CN)_2$.[4] However the reaction of $(C_6H_5)SiH_2CN$ with BF_3, *en route* to '$B(CN)_3$', produced an amorphous sp^2 hybridized B–C–N solid which was crystallized at 750 °C and 100 kbar to yield a two-dimensional graphite-like structure. The resultant B–C–N compositions have attracted considerable attention in the field of materials science because they are expected to have novel and useful properties as semiconductors with tunable bandgaps intermediate to those of graphite and hexagonal BN.[5]

Materials and Methods

General considerations

Reactions were performed under pre-purified N_2 using standard Schlenk and drybox techniques. **Caution:** manipulations involving cyanides and azides should be performed with the utmost care. Distillation and sublimation of silyl and group III cyanides should always be performed in a well-ventilated fume hood and behind protective shielding (especially for azido compounds). Solvents were distilled from sodium benzophenone ketyl under N_2 prior to use. ^1H-NMR and ^{13}C-NMR spectra were recorded on Varian Gemini 300, Varian Unity 400 and 500 spectrometers. FTIR spectra were recorded on a Nicolet-Magna IR 550 spectrometer either as a Nujol mull between KBr plates or in a 10 cm gas cell with KBr windows. Electron-impact mass spectra were performed on a Finnigan-MAT model 312 mass spectrometer (IE = 70 eV, source temperature = 225 °C) in the ASU departmental mass spectrometry facility. Elemental analyses were performed by Desert Analytics (Tucson, AZ, USA). The starting materials $(C_6H_5)SiH_2Cl$, *p*-(tolyl)SiH_2Cl, LiN_3 and LiCN were prepared according to literature procedures. NaN_3 (Aldrich, 99.5%) was heated under vacuum for 10 h prior to use. Others, such as Me_3SiCN (Gelest, 95%), were prepurified by trap-to-trap distillation prior to use, while $BeCl_2$ (Alfa Aesar, 99%), BBr_3 (Alfa Aesar, 99%), BF_3 (Air Liquide, 99.5%), $AsCl_3$ (Aldrich, 99%), $AsBr_3$ (Aldrich, 99%), $GaCl_3$ (Aldrich, 99%) and $GaBr_3$ (Aldrich, 99%) were used as received.

Synthesis of Cl_2AsN_3

A 200 ml Schlenk flask was charged with 1.26 g NaN_3 (19.3 mmol) and 80 ml acetonitrile. Subsequently, 3.20 g $AsCl_3$ (17.7 mmol) was syringed into the NaN_3–acetonitrile mixture and within several minutes a yellow solution was formed. After refluxing for 7 h at 85 °C a colorless solid was produced, and the mixture was filtered and then distilled through traps held at −3, −25, and −196 °C. The −3 °C trap contained predominately Cl_2AsN_3 and traces of unreacted $AsCl_3$, while the −25 °C trap contained pure $AsCl_3$. The contents of the −3 °C trap were separated by fractional distillation to obtain pure Cl_2AsN_3 (1.8 g, 54% yield) as a clear, colorless liquid with a vapor pressure of 2.5 Torr at 22 °C. IR (gas, cm^{-1}): 2422 (vs), 1219 (s), 673 (w), 570 (vw), 488 (m), 393 (s). EIMS (*m/e*): isotopic envelopes centered at 187 (M^+), 154 ($ClAsN_3{}^+$), 145 (Cl_2As^+), 124 ($ClAsN^+$), 110 ($ClAs^+$), 89 (AsN^+), 75 (As^+), 35 (Cl^+), 42 ($N_3{}^+$), 28 ($N_2{}^+$), 14 (N^+).

Synthesis of Br_2AsN_3

A 200 ml Schlenk flask was charged with 1.34 g NaN_3 (20.6 mmol) and 80 ml acetonitrile. Subsequently, 5.2 g of $AsBr_3$ (16.5 mmol) was syringed into the NaN_3–acetonitrile mixture and within several minutes a yellow solution was formed. After refluxing for 6 h at 85 °C a colorless solid was produced. The mixture was filtered and then vacuum distilled through −5, −25, −196 °C traps. Pure Br_2AsN_3 was obtained in the −5 °C trap as a colorless liquid which exhibited a vapor pressure of 0.2 Torr at room temperature (3.66 g, 80% yield). The characterization was conducted by IR as well as first principle simulations of the vibrational properties (see below). IR (gas, cm^{-1}): 2119 (vs), 1219 (s), 664 (w), 564 (w), 480 (m).

Synthesis of $(C_6H_5)SiH_2N_3$

To a slurry of 2.5 g of LiN_3 (51.0 mmol) in 20 ml of benzene was added 7.0 g of $(C_6H_5)SiH_2Cl$ (49.0 mmol) dissolved in 20 ml of benzene and the resulting mixture was stirred for 18 h at room temperature and then filtered. The filtrate was distilled at 80 °C at atmospheric pressure to remove the solvent. The remainder of the liquid was distilled at 75 °C at 1 Torr to yield pure $(C_6H_5)SiH_2N_3$. Yield: 4.8 g (66%). Anal. calcd for $C_6H_7N_3Si$: C, 48.4; H, 4.7; N, 28.1. Found: C, 48.8; H, 4.5; N, 27.2. IR (film, cm^{-1}): 3445 (w, br), 3078 (m), 3066 (m), 3022 (m), 2619 (w, br), 2144 (vs, br), 1963 (w), 1891 (w), 1823 (w), 1777 (w), 1596 (m), 1493 (w), 1436 (s), 1333 (s, br), 1131 (s), 941 (s, br), 873 (vs, br), 744 (m), 695 (s), 610 (s), 568 (m), 470 (m), 393 (m). ^1H-NMR (C_6D_6, δ): 7.4–7.3 (m, 1H, PhH), 7.1–7.0 (m, 4H, PhH), 5.06 (s, 2H, SiH). ^{13}C-NMR (C_6D_6, δ): 134.8 (s), 131.4 (s), 129.0 (s), 128.6 (s). EIMS (*m/e*): isotopic envelope centered at 149 (M^+).

Synthesis of $(C_6H_5)SiH_2CN$

To a slurry of 0.25 g of LiCN (7.0 mmol) in 10 ml of benzene was added 1.0 g of $(C_6H_5)SiH_2Cl$ (6.9 mmol) dissolved in 10 ml of benzene. The resulting mixture was stirred at room temperature for 18 h, and then was filtered. The filtrate was distilled at 80 °C at atmospheric pressure to remove the solvent. The remainder of the liquid was distilled at 79 °C and 10 Torr to yield pure $(C_6H_5)SiH_2CN$. Yield: 0.75 g (81%). Anal. calcd for C_7H_7NSi: C, 62.6; H, 5.2; N, 10.4. Found: C, 62.2; H, 5.6; N, 9.0. IR (film, cm^{-1}): 3084 (m), 3058 (m), 3016 (m), 2195 (s, br), 2159 (s, br), 1968 (w), 1895 (w), 1829 (w), 1596 (w), 1549 (w), 1436 (s), 1131 (s), 1080 (s, br), 930 (s), 847 (s), 754 (m), 702 (s), 651 (m), 599 (s), 475 (m), 408 (m). ^1H-NMR ($CDCl_3$, δ): 7.7–7.6 (m, 1H, PhH), 7.6–7.4 (m, 4H, PhH), 4.67 (s, 2H, SiH). ^{13}C-NMR ($CDCl_3$, δ): 135.6 (s), 132.0 (s), 129.0 (s), 122.5 (s). EIMS (*m/e*): isotopic envelopes centered at 133 (M^+), 108 ($M^+ - CN$), and 27 (CN^+).

Synthesis of *p*-(tolyl)SiH_2CN

To a slurry of 1.70 g of LiCN (51.6 mmol) in 125 ml of benzene was added 6.79 g of *p*-(tolyl)SiH_2Cl (47.3 mmol) dissolved in 30 ml of benzene. The resulting mixture was stirred at room temperature for 18 h, and then filtered. The filtrate was distilled at 80 °C at atmospheric pressure to remove the solvent. The remainder of the liquid was distilled at 90 °C at 8 Torr as pure *p*-(tolyl)SiH_2CN. Yield: 4.80 g (78%). Anal. calcd for C_8H_9NSi: C, 65.3; H, 6.1; N, 9.5. Found: C, 64.7; H, 6.0; N, 8.6. IR (film, cm^{-1}): 3109 (w), 3070 (w), 3019 (m), 2975 (w), 2922 (m), 2866 (w), 2189 (s, br), 1916 (w), 1813 (w), 1648 (w), 1602 (s, sh), 1502 (m), 1447 (m), 1394 (s), 1380 (w), 1315 (m), 1265 (w), 1192 (w), 1115 (s, sh), 923 (s), 876 (m), 840 (s), 799 (s), 734 (w), 708 (w), 639 (m), 627 (m), 599 (s), 489 (m), 404 (m), 352 (w), 322 (w). ^1H-NMR (C_6D_6, δ): 7.08–7.05 (m, 1H, PhH), 6.79–6.77 (m, 1H, PhH), 4.06 (s, 2H, SiH), 1.92 (s, 1H, CH). ^{13}C-NMR (C_6D_6, δ): 141.3 (s), 135.0 (s), 129.0 (s), 118.6 (s), 20.9 (s). (EIMS (*m/e*): isotopic envelopes centered at 147 (M^+), 120 ($M^+ - CN$), 105 ($M^+ - CH_4$,HCN), 91 ($M^+ - H_2SiCN$), 65 ($Si_2H_6{}^+$), 52 [$(CN)_2$].

Synthesis of Br_2BN_3

To a solution of 0.31 g $(C_6H_5)SiH_2N_3$ (2.1 mmol) in 10 ml of hexane was added 0.53 g of BBr_3 (2.1 mmol) in 10 ml of hexane at −25 °C and stirred for 30 min. Upon warming to room temperature a white precipitate was slowly produced and the resultant mixture was stirred for an additional 2 h. The solvent was then removed in vacuo to obtain a colorless crystalline solid which was recrystallized either by sublimation (50 °C at 0.1 Torr) or from a hexane solution (−20 °C) to yield 0.344 g (77%). The product was identified as Br_2BN_3 using elemental analysis, IR and single crystal X-ray diffraction. BBr_2N_3: anal. calcd C, 0.0; H, 0.0; N, 19.7. Found: C, 0.8; H, 0.0; N, 19.4. IR (nujol, cm^{-1}): 2208 (vs), 1303 (w), 1240 (w), 1197 (s), 979 (s), 889 (vw), 817 (m), 771 (vw), 725 (s), 571 (m). The reaction of a hexane solution of Br_2AsN_3 with BBr_3 at −25 °C produced nearly quantitative amounts of $AsBr_3$ and a colorless solid which was characterized to be highly pure Br_2BN_3. The latter synthesis method represents a more straightforward route to pure and crystalline Br_2BN_3 product.

Table 1. Structure determination summary for Br_2BN_3

Formula	B_3 Br_6 N_9
a (Å)	9.282(10)
b (Å)	15.126(17)
c (Å)	10.989(12)
α	90.00
β	100.51(3)
γ	90.00
V ($Å^3$)	1517(3)
FW	637.98
Z	4
Space group	P 21/c
ρ_{calc} (gcm^{-3})	2.794
μ (mm^{-1})	15.873
No. observed reflections	1601
R (observed data %)	$R = 4.66$, $wR = 12.49$
R (*all data %*)	$R = 8.79$, $wR = 15.45$
a (*weight/scheme*)	0.0755

Structure of Br_2BN_3

A colorless crystal with dimensions 0.20, 0.14 and 0.08 mm was inserted in a 0.5 mm capillary tube and mounted on a Bruker SMART[7] APEX diffractometer with graphite-monochromated Mo K_α radiation. All measurements were made at room temperature and the data were processed using GEMINI[8] and SAINT.[9] An absorption correction was applied using SADABS.[10] The large value for wR_{all}(0.1545) was due to these absorption correction errors. The structure was solved using standard procedures in the SHELXTL PC[11] suite of programs. Details of the crystallographic analysis for Br_2BN_3 are listed in the Results section and representative crystallographic data are given in Table 1.

Synthesis of Cl_2GaN_3 and Br_2GaN_3 via reaction of $(C_6H_5)SiH_2N_3$ with GaX_3

A solution of 0.25 g $(C_6H_5)SiH_2N_3$ (1.7 mmol) dissolved in 5 ml of hexane was added to a solution of 0.29 g $GaCl_3$ (1.7 mmol) dissolved in 5 ml of hexane at room temperature. In the same fashion, a solution of 0.35 g $(C_6H_5)SiH_2N_3$ (2.4 mmol) dissolved in 5 ml of hexane was added to a solution of 0.70 g $GaBr_3$ (2.3 mmol) dissolved in 5 ml of hexane at room temperature. In both cases, an immediate reaction occurred which was accompanied by the formation of a white precipitate. The mixture was stirred for 18 h followed by concentration of the solution to ~1 ml. Following filtration, the white solid was washed with hexane (10 ml) and was dried in vacuum. Yields: Cl_2GaN_3 0.18 g (59%), Br_2GaN_3 0.245 g (40%). These products were identified as Cl_2GaN_3[2] and Br_2GaN_3[6] on the basis of their IR spectra and melting points.

Synthesis of $Be(CN)_2$ via reactions of *p*-(tolyl)SiH_2CN and $(C_6H_5)SiH_2CN$ with $BeCl_2$

A solution of 1.20 g *p*-(tolyl)SiH_2CN (4.05 mmol) dissolved in 25 ml of butyl ether was added to a solution of 0.270 g $BeCl_2$ (3.38 mmol) dissolved in 30 ml of butyl ether at −78 °C. Similarly a solution of 2.35 g $(C_6H_5)SiH_2CN$ (17.6 mmol) dissolved in 30 ml of butyl ether was added slowly to a stirring solution of 0.655 g $BeCl_2$ (8.2 mmol) dissolved in 40 ml butyl ether at 25 °C. In both cases a white precipitate was immediately formed upon addition of the cyanide source. The mixtures were warmed slowly to room temperature and stirred for an additional 18 h. Following filtration, the resultant solids were washed with hexane and then dried in vacuum. The crude products were subsequently heated at 500 °C for 10–18 h to yield colorless crystalline $Be(CN)_2$. Yields were: (1) *p*-(tolyl)$SiH_2CN/BeCl_2$ 0.265 g (64%); and (2) $(C_6H_5)SiH_2CN/BeCl_2$ 0.740 g (88%). IR and X-ray diffraction plots of the material matched the previously reported results for $Be(CN)_2$.[4]

Reaction of $(C_6H_5)SiH_2CN$ with BF_3

A solution of 2.50 g $(C_6H_5)SiH_2CN$ (18.8 mmol) was added to a 200 ml Schlenk flask. Subsequently, 0.305 g BF_3 (4.5 mmol) was condensed into the flask at −196 °C. The flask was slowly warmed to room temperature and a white precipitate immediately formed. The slurry was stirred for 18 h at room temperature and a dark-brown precipitate was formed. Toluene (40 ml) was added and the mixture was heated at 65 °C for 1 h. The precipitate was filtered, washed with hexanes (20 ml × 2) and dried in vacuum to obtain 0.710 g of a light brown solid. IR spectroscopy indicated a polymeric sp^2 hybridized material. Additionally, powder X-ray diffraction revealed that the solid is amorphous. This material was then heated to 250 °C for 1 h in vacuum to remove any residual organic impurities and then used in the high pressure studies as described below in the Discussion section.

Results and Discussion

$(C_6H_5)SiH_2N_3$, Br_2AsN_3 and Cl_2AsN_3

The $(C_6H_5)SiH_2N_3$ compound was prepared by the reaction of $(C_6H_5)SiH_2Cl$ with LiN_3 at room temperature as a stable colorless liquid. The starting material $(C_6H_5)SiH_2Cl$ was obtained in nearly quantitative yields by HCl chlorination of $(C_6H_5)SiH_3$ using standard literature procedures.[12] The product was readily purified by low-pressure distillation at 75 °C and 1 Torr, and was fully characterized by IR, NMR, mass spectrometry and elemental analysis. The FTIR spectrum revealed a broad and very strong band centered at 2144 cm^{-1} due to the overlapping absorptions corresponding to the asymmetric Si–H stretch of the silyl group and the asymmetric stretch of the azide ligand. The spectrum also revealed weak bands corresponding to the symmetric νN_{3sym} absorption at 1333 cm^{-1} and combination mode ($\nu N_{3as} + \nu N_{3sym}$) at 1344 cm^{-1} as well as the characteristic vibrational modes of the phenyl group. The ^1H- and ^{13}C-NMR spectra confirmed the presence of the phenyl group and also showed a strong Si–H resonance at 5.06 ppm, downshifted by 0.02 ppm with respect to the $(C_6H_5)SiH_2Cl$ starting material (5.04 ppm). Combustion analysis for C, H and N was consistent with the expected empirical formula. The mass spectrum showed the molecular ion (M^+) as the highest energy peak at 149 amu and the observed isotopic fragmentation pattern corresponded to that calculated for the compound.

The Cl_2AsN_3 and Br_2AsN_3 compounds were synthesized by reactions of NaN_3 with the corresponding arsenic halides and isolated as stable, volatile liquids readily purified by distillation and fully characterized by mass spectrometry, IR spectroscopy and first principle simulations to elucidate their structural, thermochemical and vibrational properties. The mass spectra indicate that the compounds are monomeric in the gas phase, which is consistent with their relatively high vapor pressures. This is in contrast to the group III analogs X_2MN_3 (M = B, Al, Ga, In), which are typically isolated as polymeric solids or oligomeric liquids exhibiting trimetric or tetrameric gas-phase structures.

A series of B3LYP hybrid density functional theory (DFT) simulations were carried out to corroborate the identification of Br_2AsN_3 and Cl_2AsN_3 and to predict the properties of the hypothetical analogs $HClAsN_3$ and H_2AsN_3. The latter are of interest and are included in this study because of potential applications in synthetic materials science and in particular for their use as precursors to grow mixed arsenide/nitride alloys [III–As–N alloys (III = Al, Ga, In)]. These are predicted to exhibit novel optoelectronic properties such as tunable emission in the desirable communication range of 1.2–1.7 µm. The $GaAs_{1-x}N_x$ alloys ($x = 0.02–0.05$) are highly metastable and their preparation typically requires non-equilibrium conditions including the use of nitrogen-plasma and molecular beam epitaxy. The initial fabrication of optical devices based on such materials has been demonstrated but their functionality and performance are hindered by the limited bandgap energy range and the inferior microstructural quality of the alloys. To expand the useful bandgap range and simultaneously ensure the formation of device quality materials, we envision that the single-source $HClAsN_3$ and H_2AsN_3 hydride molecules will provide a route to introduce supersaturated concentrations of the desired As and N atoms into substitutional lattice sites, leading to a wide range of metastable nitride compositions which cannot be obtained via conventional MBE routes. These compounds possess the necessary reactivity to promote maximum nitrogen incorporation via low-temperature reactions, thermodynamically driven by the elimination of stable H_2, HCl and N_2 byproducts to yield the desired As–N functionalities.

All of the above compounds adopt a similar 'dog-like' molecular structure as shown in Fig. 2. The compositional designation $XX'AsN_3$ accommodates the stoichiometries of all four compounds, Br_2AsN_3, Cl_2AsN_3 $HClAsN_3$ and H_2AsN_3, with $\{X,X'\} = \{H, Cl, Br\}$. The present calculations were carried out using the Gaussian03 code at the 6-311G++(3df,3pd) level.[13]

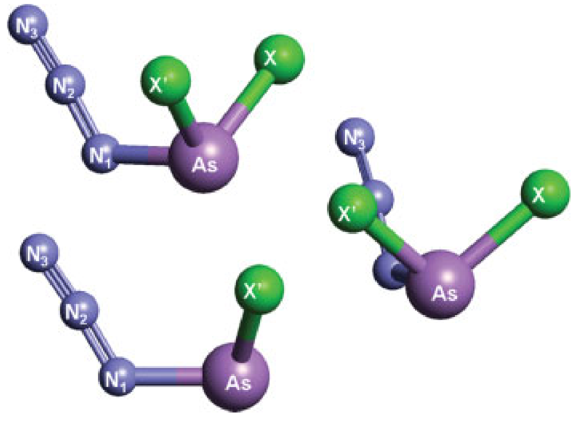

Figure 2. Generic model for the $XX'AsN_2$ molecules $\{X,X'\} = \{H, Cl, Br\}$.

Table 2. Calculated thermochemical (298 K) and structural properties of the Br_2AsN_3, Cl_2AsN_3 $HClAsN_3$ and H_2AsN_3 molecules. Electronic energies corrected for zero point energy (ZPE), thermal energy, enthalpy and free energy are also listed. Bond lengths, bond angles, dipole moments, rotational constants and energies are given in Angstroms, degrees, Debye, GHz and Hartree, respectively

	Br_2AsN_3	Cl_2AsN_3	$HClAsN_3$	H_2AsN_3
Bond lengths (Å)				
N_1-N_2	1.125	1.124	1.127	1.130
N_2-N_3	1.231	1.231	1.230	1.225
N_3-As	1.872	1.870	1.886	1.909
$As-X$	2.379	2.208	1.536	1.533
$M-X'$	2.379	2.208	2.218	1.533
Bond angles (deg)				
$N_3-N_2-N_1$	175.8	175.7	175.1	174.9
N_3-N_2-M	121.0	120.3	118.8	117.7
$X-As-X'$	99.8	98.4	92.8	91.0
$X-As-N_1$	100.7	100.2	95.5	96.7
$X'-As-N_1$	100.7	100.2	101.8	96.7
Bond torsions (deg)				
$N_3-N_2-N_1-As$	−180.0	−180.0	−177.0	−180.0
N_2-N_1-As-X	51.1	49.6	33.9	45.9
N_2-N_1-As-X'	51.1	49.6	60.1	45.9
Dipole moments (D)				
μ	1.552	1.745	2.147	2.186
Rotational constants (GHz)				
A	1.151	1.735	3.883	29.077
B	0.768	1.431	1.838	2.237
C	0.612	1.118	1.315	2.120
Energies (H)				
E_0	−7548.51010	−3320.66600	−2860.99572	−2401.32970
$E_0 + E_{ZPE}$	−7548.49540	−3320.65047	−2860.97341	−2401.30138
$E_0 + E_{th}$	−7548.48763	−3320.64317	−2860.96753	−2401.29648
$E_0 + H_{th}$	−7548.48669	−3320.64223	−2860.96659	−2401.29553
$E_0 + G_{th}$	−7548.53207	−3320.68483	−2861.00523	−2401.33035

Prior work on haloselenonyl azides $XSeO_2-N_3$ (X = F, Cl, Br)[14] using DFT B3LYP calculations and a smaller 6-311+G* basis set than that used here yielded structural and vibrational properties very similar to those obtained from a much more computationally demanding MP2 *ab initio* treatment of electron correlation effects. We therefore expect our present approach using a much more expanded basis set than 6-311+G* to provide a very quantitative description of the molecular properties.

Our simulated structural and thermochemical properties for the Br_2AsN_3, Cl_2AsN_3 $HClAsN_3$ and H_2AsN_3 molecules are presented in Table 2. For the chemically robust azide ligand, our results show that its internal bond lengths and bond angles (see below) of the $N_1-N_2-N_3$ unit are essentially molecule independent with average N_2-N_3 and N_1-N_2 bond lengths of 1.230 Å and 1.126 Å, respectively. The slightly shorter values found here in comparison to those reported in haloselenonyl azides using the same DFT approach (1.247 and 1.127 Å, respectively) can be attributed to the additional polarization functions in our basis set. Slightly larger variations are found in the As−N bond throughout the Br_2AsN_3, Cl_2AsN_3 $HClAsN_3$ and H_2AsN_3 sequence, yielding an average value of 1.88 ± 0.03 Å, but virtually identical values (1.87 Å) in the Br_2AsN_3 and Cl_2AsN_3, and a dilated value of 1.909 Å in the fully hydrated analog H_2AsN_3. The As−X bond lengths (X = H,Cl,Br) are found to exhibit the largest systematic increases with b(As−H) ≈ 1.534 Å, b(As−Cl) ≈ 2.208 Å and b(As−Br)′2.379 Å. This is virtually identical to the behavior in haloselenonyl azides,[14] where b(Se−Cl) ≈ 2.223 Å and b(Se−Br) ≈ 2.387 Å are predicted using a very similar level of theory. The calculated bond angles also exhibit well-defined trends. As expected, the $N_1-N_2-N_3$ bond angle is molecule-independent with an average value close to 176°, while the N_2-N_3-As angle becomes progressively more compact in response to the binding of Br, Cl, H atoms to the As atom due to steric effects. The largest variation in bond angle is exhibited by $X'-As-X$, which takes on values of 99.8°, 98.4°, 92.8° and 91.0° in Br_2AsN_3, Cl_2AsN_3 $HClAsN_3$ and H_2AsN_3, respectively. All molecules possessing the C_s symmetry (Br_2AsN_3, Cl_2AsN_3 and H_2AsN_3,) exhibit the expected planar configuration of $As-N_1-N_2-N_3$ (torsion angle −180°), while the torsion angle in the lower (C_1) symmetry $HClAsN_3$ is −177°, indicating a slight 3° deviation from planarity. The total dipole moments of the molecules in their equilibrium structures are also reported in the table and indicate an increasing trend along the sequence Br_2AsN_3, Cl_2AsN_3 $HClAsN_3$ and H_2AsN_3. This trend and the corresponding dipole moment magnitudes are both very similar to those recently reported for halocarbonyl azides $CXO-N_3$ (X = F,Cl,Br)[15] using the B3LYP functional and similar basis set. We also calculated the rotational constants of all molecules and find that in each case all three moments of inertia are different, indicating that all four compounds are asymmetrical tops. Finally, we list the ground state electronic energy of each molecule as well as its value corrected for zero point energy (ZPE) and the corresponding values corrected for thermal energy, enthalpy and free energy at 298K. Relative to the static ground state values, these ZPE and thermally corrected values exhibit the expected systematic increase as lighter elements are substituted on the X_1 and X_2 sites. For example, the zero-point energy correction for the H_2AsN_3 molecule is about twice that of Br_2AsN_3. Accordingly, the most desirable H_2AsN_3 species is likely to be more reactive, and thus more difficult to prepare and isolate in contrast to the heavier halide analogs.

The gas phase infrared spectra of the two synthesized Br_2AsN_3 and Cl_2AsN_3 molecules are compared with the DFT simulated counterparts in Fig. 3. The key features are labeled $\nu_1-\nu_8$ in the simulated spectra where all the vibrational modes are present. The experimental spectra were recorded at room temperature using a fraction of the compounds vapor pressure. The corresponding gas phase theoretical spectra were computed using the usual harmonic normal mode analysis on the ground state equilibrium structure, obtained using tight convergence criteria at the B3LYP/6-311++(3df,3pd) level. The calculated normal mode frequencies of both Br_2AsN_3 and Cl_2AsN_3 were all positive, indicating that the corresponding ground state structures are dynamically stable. The comparisons shown in Fig. 3 indicate an excellent general agreement between the observed and simulated data. In these plots, the simulated spectra are separated into low- and high-frequency segments, as indicated by the top trace and bottom trace on each panel, respectively. We found that a scale factor of 0.95 was required to reconcile these with the experimental values (no scaling was necessary in the low frequency range). The high-frequency scale factor differs significantly from the typical value 0.979 derived in our

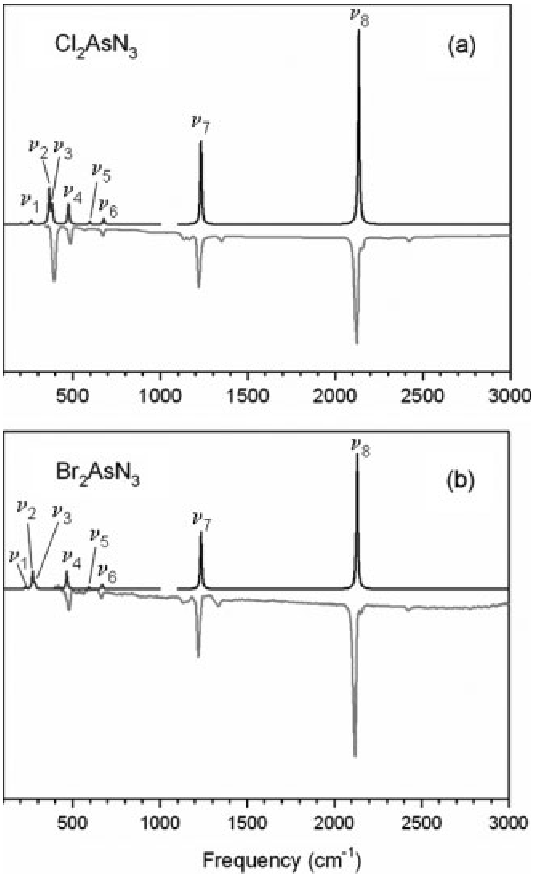

Figure 3. Comparisons of the calculated (top trace) and observed (bottom trace) room temperature IR spectra for Cl_2AsN_3 (a) and Br_2AsN_3 (b). A frequency scale factor of 0.95 was applied to the calculated high-frequency spectra.

prior work using the same DFT approach in Si–Ge hydride molecules and mixed halogen/hydride analogs.[16–18] It should be noted that the scale factor 0.95 used here is similar to the 0.96 value used previously in studies of dimethylaluminum azide clusters.[19]

A summary of the main spectral features and mode assignments for the Br_2AsN_3 and Cl_2AsN_3 molecules is provided in Table 3. The most prominent peaks in both molecules (labeled ν_7 and ν_8 in Fig. 3) occur near 1220 and 2120 cm^{-1} and correspond to symmetric and asymmetric N–N–N stretches, respectively. The corresponding N–N–N bending modes perpendicular and parallel to the saggital N–N–N–As plane occur near 596 and 673 cm^{-1} in the simulated spectra of both molecules. The more intense of these is the parallel N–N–N bending mode, which is seen at 662 and 674 cm^{-1} in Br_2AsN_3 and Cl_2AsN_3, respectively. The normal mode designated ν_4 occurring in the ~470–490 cm^{-1} range in both molecules corresponds to stretching between the As atom and the N–N–N unit. We note that this latter mode is observed, and calculated, to occur at a frequency approximately 8 cm^{-1} higher in Cl_2AsN_3 than in Br_2AsN_3 analog. The lowest frequency mode, denoted by ν_1, is predicted to occur at 231 and 262 cm^{-1} in Cl_2AsN_3 and in Br_2AsN_3 respectively, and corresponds to a wagging motion of the N–N–N group relative to the As atom. Finally, the most Cl- and Br-specific modes correspond to asymmetrical and symmetrical X–As stretching motions which are denoted as ν_2 and ν_3, respectively. Theoretically, these are predicted to differ by ~100 cm^{-1} in the Br_2AsN_3 and Cl_2AsN_3 molecules.

$(C_6H_5)SiH_2CN$ and *p*-(tolyl)SiH_2CN

The $(C_6H_5)SiH_2CN$ compound was synthesized by reaction of $(C_6H_5)SiH_2Cl$ with LiCN as a mobile colorless liquid, which is distilled readily at 79 °C and 10 Torr. Its identity was established by spectroscopic methods and elemental analysis. The IR spectrum revealed the presence of C–N and Si–H stretching modes with broad overlapping peaks at 2195 and 2160 cm^{-1}, respectively. The -SiH_2CN moiety is also evident in the NMR spectra. The ^1H and ^{13}C resonances of Si–H and C–N appear at δ 4.67 and δ 122.5, respectively. Elemental analysis for C, H and N is in agreement with the empirical formula of the compound. The mass spectrum showed isotopic envelops centered at 133 (M^+), 108 (M^+ − CN) and 27 (HCN^+), which are also consistent with the $(C_6H_5)SiH_2CN$ formula.

The *p*-(tolyl)SiH_2CN compound was prepared in a similar manner to the previous method and was isolated as a mobile, colorless liquid, which was purified by distillation at 90 °C and 8 Torr. The IR spectrum showed a rather broad absorption band centered at 2190 cm^{-1}, which corresponds to an overlap of the ν_{as}(C–N) and ν_{as}(Si–H) vibrational peaks. The ^{13}C-NMR spectrum revealed a weak resonance at δ 118.6 ppm attributed to the cyano carbon and the ^1H spectrum showed the Si–H resonance at 4.06 ppm, with all the resonances expected from the tolyl group (see experimental section above). The mass spectrum and C, H and N combustion

Table 3. Vibrational frequencies and mode assignments for the X_2AsN_3 molecules. High frequencies have been scaled by a factor of 0.95

	Br_2AsN_3		Cl_2AsN_3		
Low Frequency	*Theory*	*Exp*	*Theory*	*Exp*	*Mode Assignment*
ν_1	231		262		‘N_3’–As wagging
ν_2	269		365		Asymmetrical X–As stretching
ν_3	285		381	391	Symmetrical X–As stretching
ν_4	466	478	474	486	‘N_3’–As stretching
ν_5	595		597		N_3 bending ⊥ to ‘N_3’–As plane
ν_6	670	662	677	674	N_3 bending || to ‘N_3’–As plane
High Frequency					
ν_7	1235	1219	1231	1218	Symmetric N_3 stretching
ν_8	2130	2118	2134	2122	Asymmetric N_3 stretching

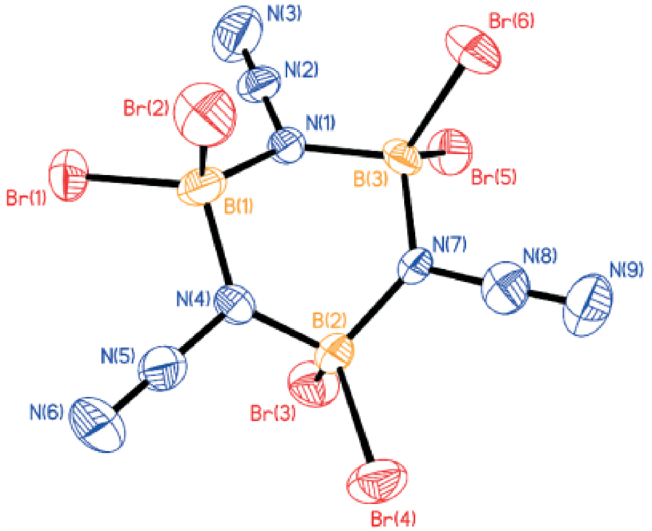

Figure 4. Molecular structure of $(Br_2BN_3)_3$.

results are consistent with the empirical formula of the title compound.

Reactions of $(C_6H_5)SiH_2N_3$ and Br_2AsN_3 with Ga and B halides

The reaction of $(C_6H_5)SiH_2N_3$ with $GaCl_3$ or $GaBr_3$ in hexane immediately produced Cl_2GaN_3 and Br_2GaN_3 precipitates, respectively, in high yields. These solids were initially characterized by IR and were found pure to be devoid of any residual organic groups. No evidence of adduct formation was observed in solution or in the precipitated solid, indicating that intermediates such as $MX_3 \bullet (C_6H_5)SiH_2N_3$ are likely to be unstable relative to those of Me_3SiN_3. Accordingly, the $(C_6H_5)SiH_2N_3$ species appears to be a much better azide ligand donor than Me_3SiN_3, presumably due to the presence of a more electropositive Si center. The reactions of $(C_6H_5)SiH_2N_3$ as well as Br_2AsN_3 with BBr_3 in hexane also resulted in the direct formation of pure Br_2BN_3 in high yields. There was no indication of any adduct formation either in solution or in the solid state. In the reactions involving Br_2AsN_3, a quantitative amount of $AsBr_3$ was recovered and used to regenerate the Br_2AsN_3 starting material. The high yield and purity of the final product clearly indicates that the reaction of Br_2AsN_3 with BBr_3 represents a much-improved synthetic route to the formation of Br_2BN_3 over the previous method utilizing Me_3SiN_3. The high material purity was determined by combustion analysis and confirmed by IR spectroscopy, indicating complete absence of any organic impurities.

Br_2BN_3 samples were recrystallized from hexane or by slow sublimation at 50 °C to form colorless blocky crystals, which were then used to obtain a single crystal structure of the material by XRD. A representation of the molecular structure is shown in Fig. 4, indicating that the compound is trimeric in the solid state. The trimer comprises a hexagonal B_3N_3 core with cyclohexane-like structure containing B–N–B linkages. The $(Br_2BN_3)_3$ hetero-cycle is formed by three boron atoms bridged by the α-nitrogens of the azide groups while the non-bridged positions are occupied by up and down bromine atoms. The bonding parameters of the compound are listed in Table 4. The average angle about the boron center is close to 110–111°, indicating a slight distortion from tetrahedral coordination. The azide bond angles and lengths are typical of those reported for other group 13 azido compounds.[20] The bond angle N–N–N angles are in the range 176.1–178.8°, indicating that the N_3 ligand is nearly linear. The bond distances N1–N2 (1.277 Å), N4–N5 (1.259 Å) and N7–N8 (1.259 Å) are substantially longer than the corresponding terminal counterparts N2–N3 (1.072 Å), N5–N6 (1.111 Å) and N8–N9 (1.118 Å). The B–N and B–Br bond lengths range from 1.556–1.580 and 1.977–1.994 Å, respectively, and appear to be similar to those reported for $(Cl_2BN_3)_3$.[21]

Table 4. Selected bond distances (Å) and bond angles (deg)

Bond distances	
B1–Br1	1.977(14)
B1–Br2	1.986(15)
N1–N2	1.277(14)
N2–N3	1.072(14)
N1–B1	1.580(15)
N1–B3	1.556(14)
N4–B1	1.567(15)
Bond angles	
N2–N1–B1	113.9(8)
N2–N1–B3	116.0(9)
B3–N1–B1	129.0(9)
N1–N2–N3	176.1(12)
N4–N5–N6	178.0(14)
N7—N8–N9	178.8(13)
N4–B1–N1	102.2(8)
Br1–B1–Br3	111.6(6)
N1–B1–Br1	110.9(9)
N1–B1–Br2	110.6(8)

Reactions of $(C_6H_5)SiH_2CN$ and *p*-(tolyl)SiH_2CN with halides of Be and B

In order to determine whether the same electronic tuning of Si could result in enhanced cyanide transfer to group II and III elements, reactions of $BeCl_2$ and BF_3 were carried out with $(C_6H_5)SiH_2CN$, *p*-(tolyl)SiH_2CN and Me_3SiCN. The utility of $(C_6H_5)SiH_2CN$, as an improved CN donor was indeed confirmed by higher product yields of crystalline $Be(CN)_2$ in comparison to earlier synthetic methods in which Me_3SiCN was used. Additionally, the X-ray diffraction pattern of $Be(CN)_2$ was found to be identical to the previously reported pattern.[4] The use of *p*-(tolyl)SiH_2CN as a C–N source for the formation of $Be(CN)_2$ led to lower than expected product yields, even in comparison to $(CH_3)_3SiCN$. This could be attributed to the electron-donating *para* methyl group of the phenyl ligand, which results in an inductive effect that renders Si more electron-rich and less susceptible to nucleophilic attack. The ^{13}C NMR data supports this claim in which the cyano carbon of *p*-(tolyl)SiH_2CN is more shielded and shifted up-field in comparison to the cyano carbon peak of $(C_6H_5)SiH_2CN$.

The reaction of $(C_6H_5)SiH_2CN$ with BF_3 proceeds via elimination of $(C_6H_5)SiH_2F$ to yield a brown solid containing B, C and N in accordance with the reaction illustrated by eqn (2) below.

$$BF_3 + 3(C_6H_5)SiH_2CN \longrightarrow \text{`}BC_3N_3\text{'} + 3(C_6H_5)SiH_2F \tag{2}$$

Transmission electron microscopy (TEM) and powder X-ray diffraction analysis revealed that the product comprised of small particles that appeared to be almost completely amorphous. The

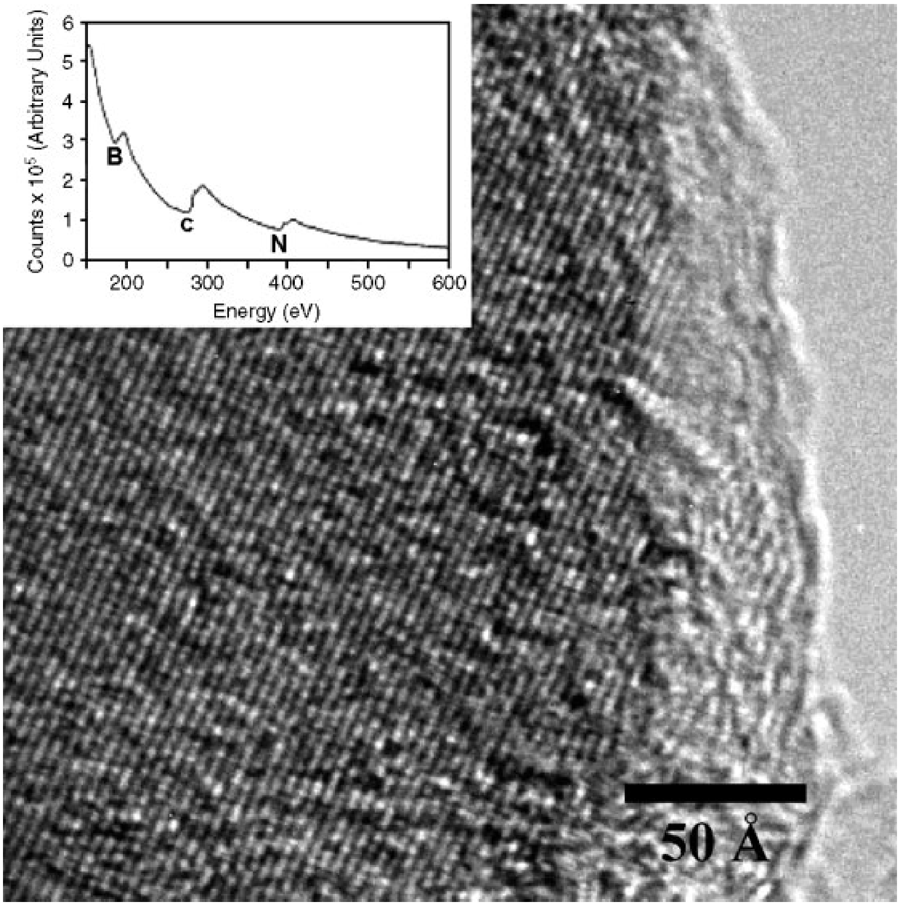

Figure 5. Electron micrograph of graphite-like B–C–N lattice fringes. (Inset) EELS spectrum of corresponding crystallite indicating sp^2 hybridized B–C–N.

infrared spectrum indicated the presence of an sp^2 hybridized planar network similar to that of amorphous carbon. In contrast, the reaction of BF_3 with Me_3SiCN yielded polycrystalline Lewis acid–base compounds with the molecular formula $(Me_3SiCN) \bullet B(CN)_{3-x}F_x$ ($x = 0$–3). Nevertheless, complete exchange of F by CN proceeds with direct formation of B–C–N polymers rather than the molecular species, suggesting that this compound is a more effective CN source than Me_3SiCN. A brief survey of preliminary high pressure experiments at 750 °C and 100 kbar using amorphous B–C–N resulted in formation of a polycrystalline solid with platelet-like morphology and homogeneous size distribution. High-resolution TEM and electron diffraction analyses indicated a graphite-like structure with lattice parameters similar to graphite and hexagonal BN. Figure 5 is a high-resolution image showing graphite-like lattice fringes of a typical crystallite. The EELS spectrum (Fig. 5 inset) indicated that the crystallites contain sp^2 hybridized C, B and N. The near-edge fine structure of the K-shell ionization edges of the elements showed π to π^* transitions similar to those of graphitic BN and elemental C. The TEM and EELS data suggest that the high-pressure product is a true B–C–N solid solution between carbon and boron nitride.

Conclusion

A new family of cyanide and azide delivery compounds has been synthesized, including Cl_2AsN_3, Br_2AsN_3, $(C_6H_5)SiH_2N_3$, $(C_6H_5)SiH_2CN$ and *p*-(tolyl)SiH_2CN, which are shown to react readily with metal halides to produce useful precursors for the subsequent deposition of optoelectronic nitrides and the formation of porous cyanide framework solids. Reactions involving the Cl_2AsN_3 and Br_2AsN_3 analogs proceed via elimination of the corresponding halides, which are fully recovered and then used to regenerate the parent compounds, indicating that these species represent a catalytic delivery source of N_3. *Ab initio* methods were used to elucidate the structural and spectroscopic properties of the arsenic compounds and their hypothetical H_2AsN_3 and $HClAsN_3$ analogs, which are of particular interest for applications in the growth of a new composition range of mixed As–N semiconductor alloys. The results indicated that H_2AsN_3 is likely to be more reactive, and thus more difficult to prepare and isolate in contrast to the heavier halide analogs.

Acknowledgments

This work was supported by the National Science Foundation. We thank Dr. Tolle for obtaining the electron microcopy images.

References

[1] D. A. Neumayer, J. G. Ekerdt, *Chem. Mater.* **1996**, *8*, 9; b) J. Kouvetakis, J. McMurran, C. Steffek, T. L. Groy, J. L. Hubbard, L. Torrison, *Main Group Metal Chem.* **2001**, *24*, 77; c) R. A. Fischer, A. Devi, *Rec. Res. Devl. Crystal Growth Res.* **2000**, *2*, 61; d) J. Kouvetakis, J. McMurran, C. Steffek, T. L. Groy, J. L. Hubbard. *Inorg. Chem.* **2000**, *39*, 3805; e) J. Kouvetakis, J. McMurran,

C. Steffek, T. L. Groy, J. L. Hubbard, *Inorg. Chem.* **2000**, *39*, 3805; f) D. J. Williams, J. Kouvetakis, M. O'Keeffe, *Inorg. Chem.* **1998**, *37*, 4617; g) D. J. Williams, D. E. Partin, F. J. Lincoln, J. Kouvetakis, M. O'Keeffe, *J. Solid State Chem.* **1997**, *134*, 164; h) D. J. Williams, B. Pleune, J. Kouvetakis, M. D. Williams, R. A. Andersen, *J. Am.Chem. Soc.* **2000**, *122*, 7735.

[2] J. Kouvetakis, J. McMurran, P. Matsunaga, M. O'Keeffe, *Inorg. Chem.* **1997**, *36*, 1792.

[3] J. McMurran, J. Kouvetakis, D. C. Nesting, D. J. Smith, J. L. Hubbard, *J. Am. Chem. Soc.* **1998**, *120*, 5233.

[4] D. Williams, B. Pleune, K. Leinenweber, J. Kouvetakis, *J. Solid State Chem.* **2001**, *159*, 244.

[5] M. Kawaguchi, *Adv. Mater.* **1997**, *9*, 615; b) B. Rand, A. V. K. Westwood, in *Design and Control of Structure of Advanced Carbon Materials for Enhanced Performance* (Eds.: B. Rand, *et al.*). Kluner Academic: Dordrecht, **2001**, 319.

[6] J. McMurran, D. Dingguo, K. Balasubramanian, C. Steffek, J. Kouvetakis, *Inorg. Chem.* **1998**, *37*, 6638.

[7] SMART, Program for collecting single crystal X-ray Diffraction Data from 2 dimensional detectors. Bruker Analytical X-ray Instruments Inc., Madison, WI, **2001**.

[8] GEMINI, Program for separating multiple crystal X-ray diffraction data from 2-dimensional detectors. Bruker Analytical X-ray Instruments Inc., Madison, WI, **2001**.

[9] SAINT, Program for integrating single crystal X-ray diffraction data from 2-dimensional detectors. Bruker Analytical X-ray Instruments Inc., Madison, WI, **2001**.

[10] R. H. Blessing, SADABS, Program for absorption correction using SMART CCD based on the method of Blessing. *Acta Crystallogr.* **1995**, *A51*, 33.

[11] G. M. Sheldrick, SHELXTL PC Version 5.1, an integrated system for solving, refining, and displaying crystal structures from diffraction data. Bruker Analytical X-Ray Instruments Inc., Madison, WI, **1997**.

[12] J. Zech, H. Schmidbaur, *Chem. Ber.* **1990**, *123*, 2087.

[13] *Gaussian 03*, Revision B. 04, M.J. Frisch *et al*. Gaussian, Inc., Pittsburgh PA, **2003**.

[14] W. Forner, H. M. Badawi, Z. S. Seddigi, *Int. J. Mol. Sci.* **2005**, *6*, 230.

[15] H. M. Badawi, W. Forner, K. S. Al-Ghamdi, *J. Mol. Model.* **2003**, *9*, 124.

[16] J. B. Tice, A. V. G. Chizmeshya, R. Roucka, J. Tolle, B. R. Cherr, J. Kouvetakis, *J. Am. Chem. Soc.* **2007**, *129*, 7950.

[17] A. V. G. Chizmeshya, C. J. Ritter, C. Hu, J. B. Tice, J. Tolle, R. A. Nieman, I. S. T. Tsong, J. Kouvetakis, *J. Am. Chem. Soc.* **2006**, *128*, 6919.

[18] C. J. Ritter, C. Hu, A. V. G. Chizmeshya, J. Tolle, D. Klewer, I. S. T. Tsong, J. Kouvetakis, *J. Am. Chem. Soc.* **2005**, *127*, 9855.

[19] Q. Y. Xia, H. M. Xiao, X. H. Ju, X. D. Gong, *Chin. J. Chem.* **2004**, *22*, 1245.

[20] D. A. Neumayer, A. H. Cowley, A. Decken, R. A. Jones, V. Lakhoita, J. G. Ekerdt, *J. Am. Chem. Soc.* **1995**, *117*, 5893; b) A. C. Frank, F. Stowasser, H. Sussek, H. Pritzkow, C. R. Miskys, O. Ambacher, M. Giersig, R. A. Fisher. *J. Am. Chem. Soc.* **1998**, *10*, 2041; c) C. J. Carmalt, A. H. Cowley, R. D. Culp, R. A. Jones, *Chem. Commun.* **1996**, *12*, 1453.

[21] V. U. Mueller, *Z. Anorg. Allg. Chem.* **1971**, *382*, 110.